SIAM J. SCI. COMPUT.
Vol. 32, No. 4, pp. 1913–1928

SMOOTHNESS AND CONVEX AREA FUNCTIONALS—REVISITED*

P. BARRERA SÁNCHEZ†, J. J. CORTÉS†, F. J. DOMÍNGUEZ-MOTA‡, G. GONZÁLEZ FLORES†, AND J. G. TINOCO-RUIZ‡

Abstract. In this paper, we introduce two new functionals within the context of the variational grid generation problem: an area functional and a smoothness functional. Both of them are based on an improved adaptive algorithm which focuses on the most folded grid cells. It is shown that when they are minimized in order to generate smooth and convex grids on irregular planar regions the optimization process converges notably faster than it does with other functionals previously reported.

Key words. numerical grid generation, direct generation method, harmonic grid, convex area functional

AMS subject classifications. 65L50, 65M50, 65N50, 78M50, 80M30

DOI. 10.1137/080745171

1. Introduction.

One way to generate convex and smooth structured grids over irregular regions in the plane consists of minimizing an appropriate functional: this is the main idea of variational grid generation [9]. It has been studied in detail in several papers, and there is currently a robust theory regarding area and harmonic functionals, which can be used for successfully gridding irregular regions [5, 6, 7, 8]. A deep geometric insight of these functionals is available, as presented in [4] and [2, 3, 13, 14]. Adaptive versions of all these functionals on surfaces have also been developed [1]. Two important examples of these kinds of functionals, H_ω and $S_{t,\epsilon}$, have been addressed and analyzed in [1, 2, 4].

Considering the results presented in these papers, which pose a whole family of functionals that can be minimized in order to generate a convex grid, it is clear that it is possible to mesh a wide variety of regions. Naturally, the next problem to be studied is whether it is possible to speed up the corresponding optimization process. In this paper, we present a new parameter update which combines the robustness of the algorithm for H_ω and the speed of the adaptive smoothness functional described in [14]; the acceleration in the generation procedure is illustrated through several examples.

This paper is organized as follows: section 2 includes the basic notation, and section 3 addresses ϵ-convexity and the direct grid generation problem. Sections 4, 5, and 6 present a brief review of the previous functionals H_ω and $S_{t,\epsilon}$. Sections 7 and 8 introduce the new functionals based on the accelerated adaptive algorithm. Section 9

*Received by the editors December 29, 2008; accepted for publication (in revised form) April 26, 2010; published electronically July 1, 2010. This work was supported by Intercambio Académico of UNAM and grant CONACyT DAIC 83415, "Generación numérica de mallas empleando el método variacional directo y algunas aplicaciones."
http://www.siam.org/journals/sisc/32-4/74517.html

†Facultad de Ciencias, U.N.A.M., Mexico City 04800, Mexico (pbs@hp.fciencias.unam.mx, jjcaa1@gmail.com, gfgf@hp.fciencias.unam.mx). The work of these authors was supported by the Macroproyecto: Tecnologías para la Universidad de la Información y la Computación.

‡Facultad de Ciencias Físico Matemáticas, U.M.S.N.H., Morelia, Michoacán 58060, Mexico (dmota@umich.mx, jtinoco@umich.mx). The work of these authors was supported by CIC-UMSNH grant 9.16, "Complejidad numérica y computacional de la solución numérica de ecuaciones diferenciales parciales y algunas aplicaciones I y II," and grant CONACyT DAIC 83415, "Generación numérica de mallas empleando el método variacional directo y algunas aplicaciones."

presents the numerical tests and comparisons in a battery of quite irregular regions. As expected, conclusions in section 10 end this paper.

2. Notation. The regions for the problem of interest here are simply connected domains Ω in the plane whose boundaries are closed polygonal Jordan curves with positive orientation. For such regions, the grid generation problem can be described as the construction of continuous functions $x(\xi,\eta)$, $y(\xi,\eta)$, which define one-to-one mappings

$$\mathbf{x} : R \mapsto \Omega \quad \text{with } \mathbf{x} = (x(\xi,\eta), y(\xi,\eta))$$

from the unit square

$$R = \{(\xi,\eta) | 0 \le \xi \le 1,\ 0 \le \eta \le 1\}$$

onto the physical region Ω and satisfy $\mathbf{x}(\partial\mathbf{R}) = \partial\mathbf{\Omega}$.

In practical terms, the discrete structured grid generation problem can be described as the efficient construction of a logically rectangular subdivision of Ω into convex quadrilaterals. These subdivisions, which will be defined in the next section, will be referred to as grids.

In order to pose the definitions required for the following sections, it is important to introduce some basic definitions. Let m and n be the number of "vertical" and "horizontal" points of the region's "sides," and let Ω be the planar region defined by a Jordan polygonal curve with positive orientation γ of vertices $V = \{v_1, v_2, \ldots, v_{2(m+n-2)}\}$ (Figure 2.1).

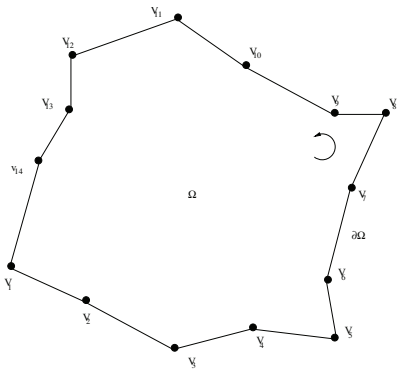

FIG. 2.1. *Example of a region defined by a simple closed polygonal curve.*

The theory addressed in this paper is valid for these particular shapes of regions. For Ω, in terms of m and n, one can see that there is a natural choice for the four "sides."

A set

$$G = \{P_{i,j} | 1 \le i \le\ m, 1 \le j \le n\}$$

of points of the plane with the fixed boundary positions given by V is called a structured, admissible, and discrete grid[1] for Ω of order $m \times n$.

[1] It has quadrilateral elements.

We say that G is convex if each one of the $(m-1)(n-1)$ quadrilaterals (or cells) $c_{i,j}$ of vertices $\{P_{i,j}, P_{i+1,j}, P_{i,j+1}, P_{i+1,j+1}\}$, $1 \le i < m$, $1 \le j < n$, is convex and nondegenerate.

Let c be an oriented quadrilateral of vertices $\{PQRS\}$. The latter defines four oriented triangles, $\triangle^{(1)} = \triangle(SPQ)$, $\triangle^{(2)} = \triangle(PQR)$, $\triangle^{(3)} = \triangle(QRS)$, and $\triangle^{(4)} = \triangle(RSP)$ (Figure 2.2). In what follows, it will be of the greatest relevance to consider that every grid cell $c_{i,j}$ is divided into four triangles $\{\triangle_{i,j}^{(k)}, k = 1, \ldots, 4\}$ in this same way.

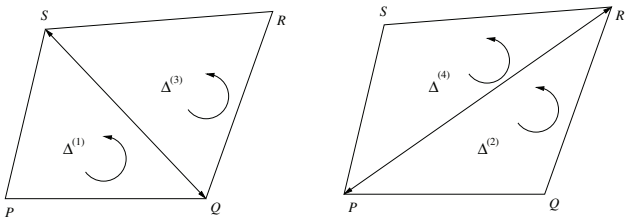

FIG. 2.2. *The four oriented triangles defined by a quadrilateral grid cell.*

Thus, the orientation of the boundary not only induces that of the cells and their triangles but also assigns a sign on the areas of the triangles, which is the main key for determining whether a grid is convex.

In this context, we introduce two basic triangle-dependent quantities: λ and α. For the oriented triangle with vertices $A, B, C \in \mathbb{R}^2$, these functions are defined as

$$\lambda(\triangle(A,B,C)) = \|A-B\|^2 + \|C-B\|^2, \tag{2.1}$$

where $\overline{AB}$ and $\overline{CB}$ are cell sides and

$$\alpha(\triangle(A,B,C)) = (B-A)^t J_2 (B-C) = 2\,\text{area}(\triangle(A,B,C)), \tag{2.2}$$

where $\|\cdot\|$ denotes the Euclidean norm and J_2 is the matrix

$$J_2 = \begin{pmatrix} 0 & 1 \\ -1 & 0 \end{pmatrix}.$$

Notice that a grid G is convex iff

$$\min\{\alpha(\triangle_q) > 0 | q = 1, \ldots, N\},$$

where $N = 4(m-1)(n-1)$ is the total number of triangles in G, considering the four triangles in each cell defined by its vertices as mentioned above.

Three useful quantities, related to α, are the following:

$$\alpha_{\_}(G) = \min\{\alpha(\triangle_q) | q = 1, \ldots, N\}, \tag{2.3}$$

$$\alpha_{+}(G) = \max\{\alpha(\triangle_q) | q = 1, \ldots, N\}, \tag{2.4}$$

$$\overline{\alpha}(G) = \frac{1}{N} \sum_{q=1}^{N} \alpha(\triangle_q). \tag{2.5}$$

An important relation can be derived from the definition of α. Since (2.2) yields

$$\sum_{q=1}^{N} \alpha(\triangle_q) = 4 \text{ Area}(\Omega), \tag{2.6}$$

we have

$$\overline{\alpha}(G) = \frac{1}{N} \sum_{q=1}^{N} \alpha(\triangle_q) = \frac{\text{Area}(\Omega)}{(m-1)(n-1)}, \tag{2.7}$$

which means that $\overline{\alpha}(G)$ actually depends only on Ω and not on a particular G.

In what follows, this value will be denoted simply as $\overline{\alpha}$. In addition, the set $M(\Omega)$ will represent the set of all the grids for Ω and, for the sake of brevity, α_q and $\alpha(\triangle_q)$ will be used indistinctly.

3. The ϵ-convexity. As we mentioned before, geometrically speaking, a grid G is convex iff $\alpha\_(G) > 0$. However, this inequality is neither scale independent nor a numerically stable test. This is due to the fact that the problem of generating convex grids in irregular regions may be ill-posed in the sense that the critical value

$$\epsilon_c(\Omega) = \max \left\{ \frac{\alpha\_(G)}{\overline{\alpha}} | G \in M(\Omega) \right\} \tag{3.1}$$

can become very small.

Nevertheless, this test can be reformulated in a numerically useful way. Since for any convex grid G we have

$$0 < \frac{\alpha\_(G)}{\overline{\alpha}} \leq \epsilon_c,$$

it follows that if we choose $\epsilon > 0$, then any grid G satisfying

$$\epsilon_c \geq \frac{\alpha\_(G)}{\overline{\alpha}} \geq \epsilon$$

is convex. Consequently, the following definition appears in a natural way.

DEFINITION 3.1. *Let ϵ be a positive number. A grid G is ϵ-convex iff*

$$\min\{\alpha(\triangle_q) > \epsilon \cdot \overline{\alpha}(\Omega) | q = 1, \ldots, N\}. \tag{3.2}$$

This new definition of convexity has proven to be very useful because it is scale independent, which is a desirable property from a numerical point of view.

The basis for the direct optimization method, as developed by Charakhch'yan and Ivanenko [7], is the minimization of a suitable function of the form

$$F(G) = \sum_{q=1}^{N} f(\triangle_q), \tag{3.3}$$

where $f(\triangle_q)$ depends only on the vertices of the triangle $\triangle_q$, and N is the total number of triangles of the grid, so our problem is to find the coordinates of the interior points of the grid G. Thus, a grid G will be represented by a point in an euclidean $2(n-1) \times (m-1)$-dimensional space where the components are the x and y coordinates of the interior points $\{P_{i,j}; 2 \leq i \leq n, 2 \leq i \leq m\}$ of the grid.

In this context, the discrete variational grid generation problem can be posed as a large scale optimization one in the following way.

PROBLEM 1. *Solve*

$$G^* = \arg \min_{G \in M(\Omega)} \sum_{q=1}^{N} f(\triangle_q)$$

over the set of admissible grids $M(\Omega)$ *for a region* Ω *and a given* ϵ *in such a way that* G^* *is* ϵ*-convex.*

As will be shown in the following sections, the key to achieving ϵ-convexity lies efficiently in the adequate selection of f.

Using (3.2), the following can be shown:

- If $\epsilon > \epsilon_c$, Problem 1 has no solution.
- In a complimentary fashion, if $\epsilon \leq \epsilon_c$, Problem 1 *has* solutions.
- If $\epsilon \approx \epsilon_c$, the problem's numerical optimization could be very difficult to solve.

4. Barrera and Tinoco's ω-functionals. The first effective functionals for the generation of convex harmonic grids on quite irregular regions were developed by Charakhch'yan and Ivanenko [7, 6]. A beautiful insight into these functionals can be found in [8].

These authors rewrote the harmonic functional proposed by Winslow [16] in a variational setting [7]. They then discretized it to obtain a function of the inner grid points given by

$$F_S(G) = \sum_{q=1}^{N} \frac{\lambda(\Delta_q)}{\alpha(\Delta_q)}, \tag{4.1}$$

which was minimized by means of a Newton-like iterative method in order to generate a harmonic grid.

It is quite easy to prove that Ivanenko's functional attains its minimum in the set of convex grids for a region due to the pole in f and the relations between α and λ [6]. However, because of the so-called barrier property, for fixed boundary points the minimization process required a rather complicated setting to get an initial convex grid [7].

Later, Tinoco-Ruiz and Barrera-Sánchez [14] developed a new smoothness functional with an easier initial setting by choosing a parameter ω that allows the use of a nonconvex initial grid. It is chosen to satisfy

$$\omega > -\alpha(\triangle_q), \quad q = 1, \ldots, N.$$

To address Tinoco's functionals, it is convenient to define the set

$$D_\omega = \{G | G \in M(\Omega), \alpha_-(G) > -\omega\}, \quad \omega \in \mathbb{R}. \tag{4.2}$$

If $\omega < \omega'$, then $D_\omega \subset D_{\omega'}$. In addition, if

$$\omega' \leq -\bar{\alpha} = -\frac{\text{Area}(\Omega)}{(m-1)(n-1)},$$

then $D_\omega = \emptyset$.

In other words, the set of values of ω such that $D_\omega \neq \emptyset$ is nonempty and bounded below. Thus, it is possible to prove the set of convex grids for Ω is nonempty: $\omega_- = glb\{k|D_\omega \neq \emptyset\} < 0$.

Let G be a grid for Ω. If $\alpha_-(G) > \omega$, then the ratio $1/(\alpha+\omega)$ is positive, so the functions

$$f_{A_\omega^{-1}}(\Delta) = \frac{1}{\omega + \alpha(\Delta)}, \quad f_{S_\omega}(\Delta) = \frac{\lambda(\Delta)}{\omega + \alpha(\Delta)} \tag{4.3}$$

are nonnegative and, as a consequence, the functionals for a grid G

$$F_{A_\omega^{-1}}(G) = \sum_{q=1}^{N} f_{A_\omega^{-1}}(\Delta_q), \quad F_{S_\omega}(G) = \sum_{q=1}^{N} f_{S_\omega}(\Delta_q) \tag{4.4}$$

are positive. Furthermore, given ω a positive number, it is possible to prove that, if $D_\omega \neq \emptyset$, both functionals $F_{A_\omega^{-1}}$ and F_{S_ω} will attain their minima in the open set D_ω [14].

By choosing a suitable initial value of ω, the iterative procedure of minimizing one of the ω-functionals and updating ω is a very efficient way to generate convex and smooth grids in a large number of planar regions. (See Figure 4.1.)

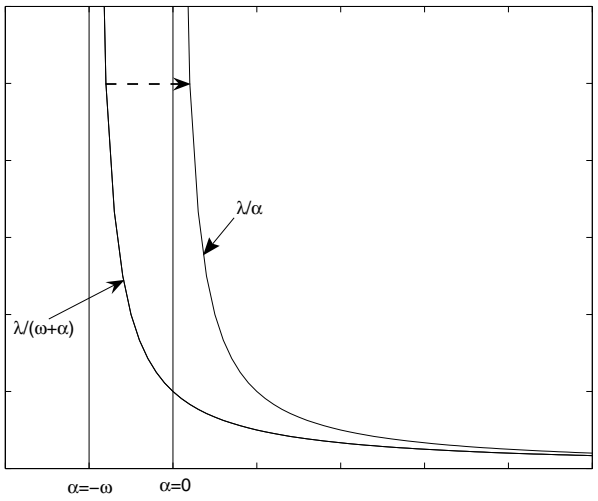

FIG. 4.1. *A sketch of the action of the parameter ω in f_{S_ω}.*

It can be summarized as follows:

1. Calculate $\alpha_-(G_0)$ for an initial grid G_0.
2. Calculate $\omega = \omega_1 \alpha_-(G_0) + \omega_2$, with suitable values ω_1 and ω_2.
3. Generate G_ω such that $F_\omega(G_\omega) = \min_{G \in D_\omega}(F_\omega(G))$.
4. Go back to step 2 until G_ω is convex.

Both functionals have very good performance in a wide range of irregular regions by focusing on the nonconvex cells of the grid. However, since they feature a pole in a neighborhood of $-\omega$, it is rather difficult to set up an automatic procedure to update

ω for very irregular regions. Therefore, it is frequently necessary to use a trial and error algorithm in order to calculate ω_1 and ω_2.

Additionally, for Ivanenko's functionals, the optimal grids generated were required only to satisfy the scale-dependent convexity test $\alpha\_(G) > 0$. This frequently caused numerical instability in some irregular regions.

5. The functional $S_{t,\epsilon}$. Ivanenko's and Tinoco-Ruiz's functionals feature poles as barriers, a fact that can be disadvantageous and the cause of instability if small values of α are produced on some irregular regions. In order to avoid the use of poles as barriers, Barrera-Sánchez and Domínguez-Mota made a comprehensive analysis of the properties of a family of continuous discrete area functionals (i.e., with no explicit dependence on λ) with "soft" barriers to solve it [4] and proved the following theorem.

THEOREM 5.1. *Suppose that $f : \mathbb{R} \to \mathbb{R}$ is a C^2 convex, strictly decreasing, and nonnegative function, and let $F : \mathbb{R}^N \to \mathbb{R}$ be given by*

$$F(G) = \sum_{q=1}^{N} f(\alpha_q).$$

Assume that Ω is a polygonal region for which there exists a convex grid G_0. Then, it is possible to find a real number $t \geq 1$ such that the optimization problem

$$\min\{F(G)|G \in M(t\Omega)\},$$

where $t\Omega$ is the image of Ω under the mapping $x \to tx$, has a solution $\hat{G}$ that satisfies

$$\alpha\_(\hat{G}) > 0.$$

The most attractive feature of Theorem 5.1 is the fact that f must satisfy a short list of requirements. It is possible to use very economical choices in terms of flops, for instance,

$$f(\alpha) = \begin{cases} (\alpha - 1)(\alpha - 2) + 1, & \alpha < 1, \\ \frac{1}{\alpha}, & \alpha \geq 1. \end{cases} \tag{5.1}$$

However, despite its simplicity, Theorem 5.1 still lacks the scale-independent property required to work robustly on very irregular nonconvex regions. This difficulty can be overcome easily, as noted by Barrera-Sánchez et al. [2], who realized that one of the main conclusions of Theorem 5.1, the positivity of the least value of α of the optimal grid, could be restated with ease in terms of a shifted inequality.

THEOREM 5.2. *Let f and Ω be defined as in Theorem* 5.1. *Then*

$$S_{t,\epsilon}(G) = \sum_{q=1}^{N} f(t\alpha(\triangle_q) - \epsilon\overline{\alpha}(G)), \tag{5.2}$$

considered as the objective function in the optimization problem (Problem 1*), is minimized on $M(t\Omega)$ by ϵ-convex grids for a large enough $t \geq 1$.*

The ϵ-convex grids generated by minimizing $S_{t,\epsilon}$ with (5.1) have been reported in several previous papers, for instance, [4, 2]. In many very irregular regions, the presence of cells with relative large values of area has been observed. This often slows down the performance of the optimization process.

6. The functional H_w. The applicability of the ideas about the area functionals addressed in the previous sections is not limited to the generation of convex grids. Barrera-Sánchez et al. [1] proposed a new parameter-dependent smoothness functional H_w whose optimal grids are quite similar to those of $F_S(G)$ when ω is small enough.

The main idea behind this new functional consists of replacing the area function $1/\alpha$ that appears in the definition of $F_S(G)$ by a function $\varphi_\omega(\alpha)$ capable of acting as a "soft" and continuous barrier.

A natural choice for $\varphi_\omega(\alpha)$ is a continuous, convex, and strictly decreasing C^2 function identical to $1/\alpha$ for $\alpha \geq \omega$ (see [4] for details).

For instance, we can consider for a positive real number ω (see Figure 6.1)

$$\varphi_\omega(\alpha) = \begin{cases} (2\omega - \alpha)/\omega^2, & \alpha < \omega, \\ 1/\alpha, & \alpha \geq \omega. \end{cases} \tag{6.1}$$

Thus, the functional H_ω can de defined as

$$H_\omega(G) = \sum_{q=1}^{N} \lambda(\triangle_q)\varphi_\omega(\triangle_q). \tag{6.2}$$

A deeper insight into the main properties of H_ω, as well as a benchmark against the smoothness functional $F_{S_\omega}(G)$, can be found in [4].

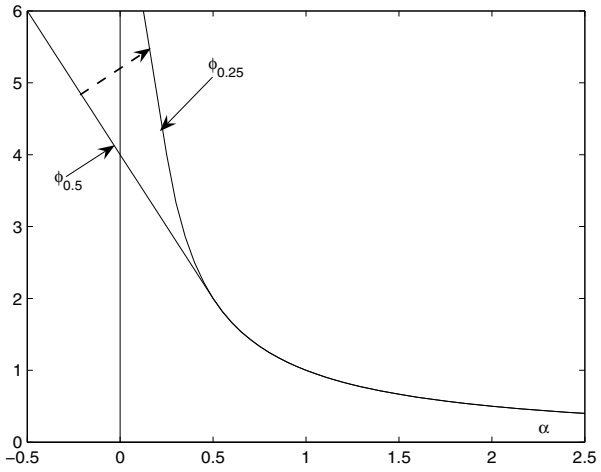

FIG. 6.1. *Sketch of the action of the parameter ω in φ_ω.*

7. The new smoothness functional. The next goal is to propose two new functionals, an area functional and a smoothness functional, both designed to take advantage of the functionals discussed so far: the efficiency and speed of the ω-functionals when acting on nonconvex cells, and the global performance of H_ω and $S_{t,\epsilon}$.

As before, this process can be done by changing the function $\varphi(\alpha)$ in H_ω. For $\alpha \geq -\omega_1 + \omega_2$, a natural replacement for this task is given by

$$\varphi_{\omega_1}(\alpha) = \frac{1}{\omega_1 + \alpha}. \tag{7.1}$$

Again, just as was done with H_ω, the "complementary" function of $\varphi_{\omega_1}(\alpha)$ for $\alpha \leq -\omega_1 + \omega_2$ is defined as the tangent to the function $1/(\omega + \alpha)$ at $\alpha_k = -\omega_1 + \omega_2$. In other words, the actual function φ is defined as

$$\varphi_{\omega_1}(\alpha; \omega 2) = \begin{cases} 1/(\omega_1 + \alpha), & \alpha \geq -\omega_1 + \omega_2, \\ (-\omega_1 + 2\omega_2 - \alpha)/\omega_2^2 & \text{otherwise}, \end{cases} \tag{7.2}$$

where ω_1 and ω_2 are parameters to be updated after the optimization step.

For H_ω, the parameter ω is updated as $\omega/2$, so it is a natural choice to update ω_2. To update ω_1, we will use a formula related to $\alpha\_$ in the current optimization step given by

$$\omega_1 = \max(-0.5 \cdot \alpha\_(G), 0), \tag{7.3}$$

for which it must be noted that the optimal grid is convex when $\omega_1 = 0$. Thus, the new smoothness functional is given by

$$H_{\omega_1,\omega_2}(G) = \sum_{q=1}^{N} \lambda(\triangle_q)\varphi_{\omega_1}(\alpha_q; \omega_2). \tag{7.4}$$

8. The new area functional. It is also possible to apply $\varphi(\alpha)$'s previous extension in order to improve the performance of the area functional $S_{t,\epsilon}$. The basic idea is to use the scaling parameter t within the function $f(\alpha)$ given by (5.1), together with the parameter ω of $F_{A_\omega^{-1}}(G)$, in order to get both effects, scaling and shifting, simultaneously. This yields the functional

$$\mathcal{S}_{t,\omega}(G) = \sum_{q=1}^{N} f(\omega + t\alpha_q). \tag{8.1}$$

In order to get the joint effect of the scaling parameter t and the adaptive pole parameter ω, the initial value of ω is set and then is halved in every iteration, while t is initially set to 1 and is doubled at the same time. When $\omega \to 0$, $\mathcal{S}_{t,\omega} \to S_{t,0}$, while as $t \to \infty$, the values of f decrease faster.

In UNAMALLA [15], these parameters are updated simply as

$$\begin{aligned} \omega &= \max(-0.35 \cdot \alpha_{min}(G), 0), \\ t &\leftarrow 2t. \end{aligned} \tag{8.2}$$

9. Numerical tests. Before testing H_{ω_1,ω_2} and $S_{t,\omega}$, it is convenient to briefly address some technical issues.

9.1. Algorithm. One can notice that the new functionals can be implemented in a simple two-loop algorithm: an outer loop for ϵ-convexity, and an inner loop to solve the optimization problem (Problem 1) numerically.

ALGORITHM. SMOOTH GRID GENERATION WITH H_{ω_1,ω_2}.

1. Choose initial values for *tolf*, *tolg* (tolerances for the function's relative change and gradient norm in the optimization process; see the following subsection), ω_2, $ITERMAX$, and $\varepsilon > 0$.
2. Generate an initial grid G_0 by transfinite interpolation [10] and scale it to satisfy $\overline{\alpha} = 1$.

3. Calculate ω_1.
4. Solve the optimization problem

$$\hat{G} = \arg \min_{G \in M(\Omega)} \{H_{\omega_1,\omega_2}(G)\} \tag{9.1}$$

until

$$\|\nabla H_{\omega_1,\omega_2}(\hat{G})\| < tolg,$$

or

$$\|H_{\omega_1,\omega_2}(\hat{G}) - H_{\omega_1,\omega_2}(G_0)\| < tolf \cdot \|H_{\omega_1,\omega_2}(G_0)\|,$$

or $ITERMAX$ has been reached.

5. If $\alpha\_(\hat{G}) > \varepsilon$, a smooth ε-convex grid has been generated and we are done; elseif $ITERMAX$ was reached, no convex grid has been found and we are done; else we update ω_1, set $G_0 \leftarrow \hat{G}$, $\omega_2 \leftarrow \omega_2/2$, and go back to step 3.

By replacing the parameters t and ω_1 and applying (8.2), this algorithm can be used with $\mathcal{S}_{t,\omega}$ instead of H_{ω_1,ω_2}. This is also true for linear convex combinations of H_{ω_1,ω_2} and $\mathcal{S}_{t,\omega}$ with other functionals.

9.2. Implementation parameters. The details of the numerical implementation of the algorithm of the previous section are the following:

1. *Scale.* In order to improve the optimization step, all the test regions were previously scaled to satisfy $\overline{\alpha} = 1$.
2. *ϵ-convexity.* For a practical implementation in the IEEE 754 double precision arithmetic, we use $\epsilon = 10^{-5}$.
3. *Initial parameters.* We set $w_2 = 0.5$ for H_{ω_1,ω_2} or $t = 1$ for $\mathcal{S}_{t,\omega}$, and $ITERMAX = 1000$.
4. *Optimization step.* The optimization is carried out by means of large-scale Newton-like methods with bound constraints: TRON [11] and L-BFGS-B [17]. The tolerances *tolf*, *tolg* are chosen as the default values for these methods.

9.3. Numerical examples. The algorithm of this section was applied to six test irregular regions that have been used frequently when testing functionals for the direct variational grid generation problem [4] (Figure 9.1):

- Havana
- Mexico
- Cat
- Great Britain
- Ucha basin
- South America

This group includes very irregular regions, for which most of the algebraic and differential methods fail, but that can be gridded successfully with the direct optimization method.

For each one of these regions, initial grids with 30, 40, and 40 points per side were generated by transfinite interpolation. In order to compare the overall performance of the new functionals, the linear combinations

$$0.5(H_{\omega_1,\omega_2}(G) + A(G)) \tag{9.2}$$

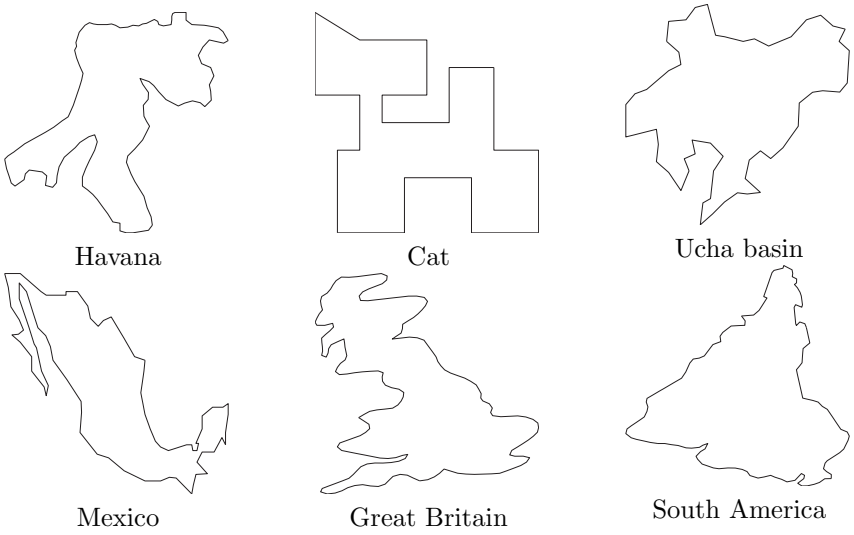

FIG. 9.1. *Test regions.*

against

$$0.5(H_\omega(G) + A(G)) \tag{9.3}$$

and

$$0.5(S_{t,\omega}(G) + L(G)) \tag{9.4}$$

against

$$0.5(S_t(G) + L(G)) \tag{9.5}$$

were used for benchmarking, where A and L are the area and length functionals [3, 5, 12] given by

$$A(G) = \sum_{q=1}^{N} \alpha(\triangle_q)$$

and

$$L(G) = \sum_{q=1}^{N} \lambda(\triangle_q),$$

respectively. All runs were performed using a personal computer with 2GbMb RAM and an Intel processor running at 1.99GHz.

For the functionals H_{ω_1,ω_2} and $S_{t,\omega}$, the parameters were updated by means of (7.3) and (8.2). For the simpler functionals H_ω and S_t, we set $\omega_1 = \omega = 0$.

In order to compare the performance of the functionals H_{ω_1,ω_2} and $S_{t,\omega}$ against H_ω and S_t, let us denote by $N(H_{\omega_1,\omega_2})$, $N(H_\omega)$, $N(S_{t,\omega})$, and $N(S_t)$ the iterations required for convergence when the functionals (9.2), (9.3), (9.4), and (9.5) are minimized, respectively. We define the performance ratios $\rho_H = N(H_\omega)/N(H_{\omega_1,\omega_2})$ and

TABLE 9.1
Comparison ratios.

Region	ρ_H	ρ_S	T_H	T_S	α_H	α_S
Hav30	0.82	1.24	0.79	1.25	1.00	3.85
Hav40	1.22	0.85	1.26	0.88	1.94	3.14
Hav50	1.27	1.12	1.26	1.15	1.37	1.41
Cat30	1.67	1.15	1.64	1.18	0.68	1.31
Cat40	1.37	1.48	1.39	1.46	0.02	0.24
Cat50	2.13	1.28	2.11	1.29	0.47	0.15
Eng30	1.25	1.07	1.28	1.08	1.21	1.03
Eng40	1.53	1.25	1.48	1.17	0.96	2.41
Eng50	1.56	0.95	1.57	0.95	0.70	1.26
Ucha30	0.91	1.47	0.88	1.46	0.28	0.38
Ucha40	0.70	1.67	0.65	1.71	0.27	1.79
Ucha50	1.20	1.67	1.13	1.73	1.28	1.80
Sud30	1.35	1.46	1.50	1.38	0.68	1.07
Sud40	0.78	1.00	1.70	1.06	0.69	0.94
Sud50	1.73	1.02	1.88	0.97	0.81	1.13
Mex30	2.33	1.23	2.23	1.28	1.08	0.01
Mex40	1.62	1.02	1.62	1.02	0.56	1.26
Mex50	1.73	1.03	1.73	1.02	1.04	1.00

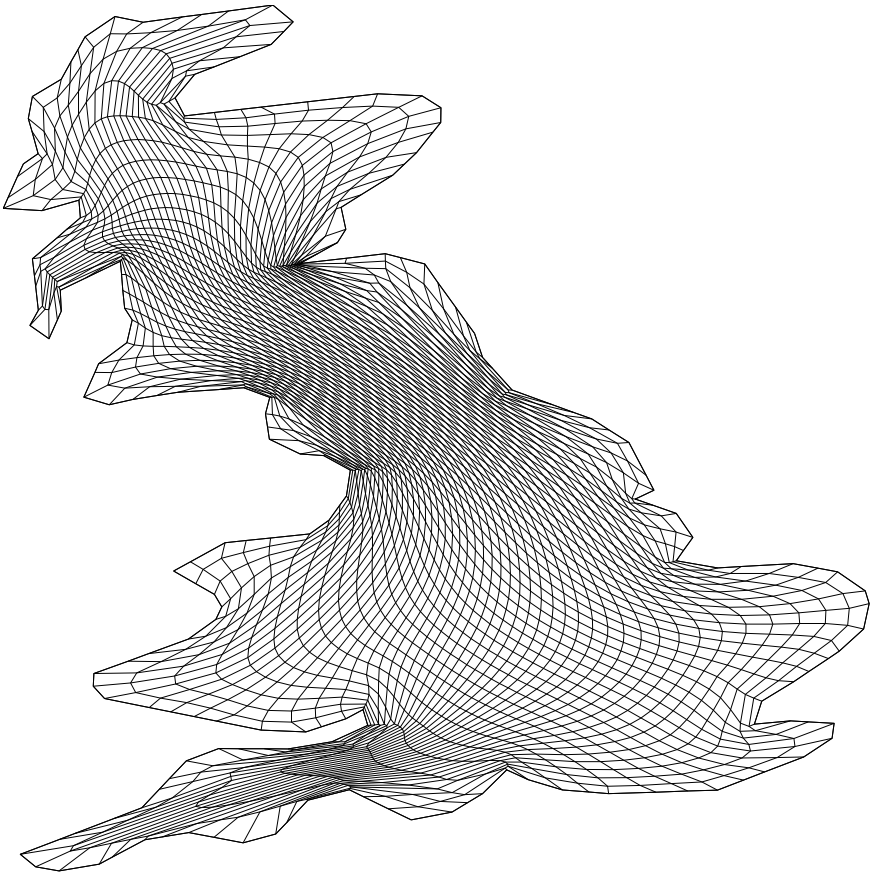

FIG. 9.2. *A grid for Great Britain with* 50 *points per side generated by minimizing* $0.5(H_{\omega_1,\omega_2}(G) + L(G))$.

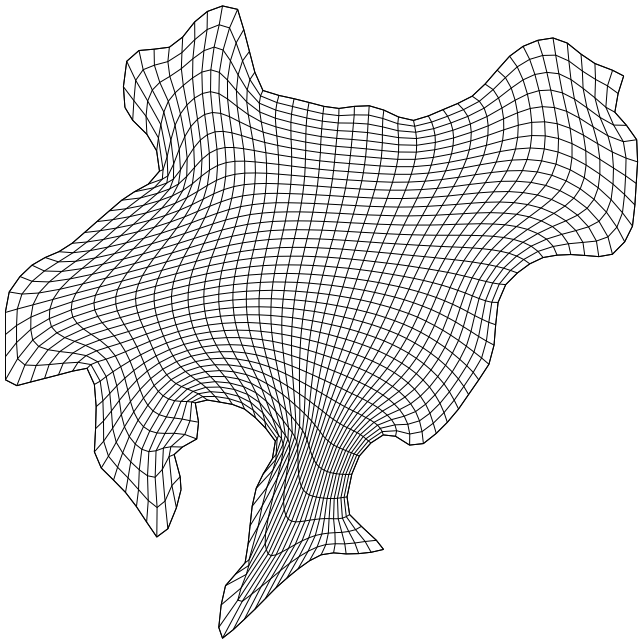

FIG. 9.3. *A grid for Ucha basin with* 40 *points per side generated by minimizing* $0.5(S_{t,\omega}(G) + L(G))$.

$\rho_S = N(S_t)/N(S_{t,\omega})$ for the number of iterations. In a similar way, we define T_H and T_S for the ratios of the elapsed time of the optimization process and α_H and α_S for the ratios of the values of $\alpha_{\_}$ in the optimal grids. Their values for the numerical tests are summarized in Table 9.1.

Two examples of the generated grids are shown in Figures 9.2 and 9.3. The effect of the double homotopic functional is quite evident: as the number of cells increases due to the increments of m and n, the optimization problem is solved faster in most of the cases, and the number of iterations and CPU time required to generate the optimal convex grid is frequently halved. This is due to the fact that the adaptive parameters ω_1 and ω have a stronger effect on the triangles with large negative areas, thus increasing the value of the barrier defined by the functionals in such a way that the optimization process can be better exploited in large problems. In 77.7% of the test cases, the new functionals H_{ω_1,ω_2} and $S_{t,w}$ are faster than H_ω and S_t.

This can be easily explained since the functionals H_ω and S_t use a global strategy to update their parameters, a strategy which is not focussed on the folded cells but on the whole grid.

10. Conclusions and future work. As noted by the numerical experiments, the main advantage of these new functionals is that they work adequately on every grid cell, and as the number of nonconvex cells decrease, they have a stronger action on the most irregular ones. In this sense, they clearly represent an improvement over the previous functionals.

Current research deals with the use of the optimal grids of the new functionals in the numerical solutions of differential equations, and the corresponding results will be reported in a future paper.

Another important problem which will be studied is the use of multioptimization

techniques as an alternative to speed up the optimization process.

Finally, it is important to mention that an implementation of these functionals is included in UNAMALLA [15], which is available for academic and research purposes.

Appendix A. Results summary. The data associated with the tests of section 9 is summarized in Tables A.1, A.2, A.3, and A.4.

TABLE A.1
Results for $0.5(H_\omega(G) + A(G))$.

Region	$\alpha\_$	$ITER$	Elapsed time
Hav30	0.08056012	50	00:31.7
Hav40	0.08918047	66	01:21.9
Hav50	0.05571226	104	03:12.5
Cat30	0.01341007	100	01:05.0
Cat40	0.00106690	103	02:00.0
Cat50	0.00819499	185	05:30.1
Eng30	0.02371219	95	01:09.4
Eng40	0.01297407	158	02:54.7
Eng50	0.00314142	200	05:55.8
Ucha30	0.00669548	42	00:25.3
Ucha40	0.01441906	46	00:48.5
Ucha50	0.05436297	59	01:41.6
Sud30	0.01327144	50	00:32.8
Sud40	0.02787514	35	01:26.5
Sud50	0.02322099	104	03:18.1
Mex30	0.00099314	469	05:07.1
Mex40	0.00059463	599	11:32.0
Mex50	0.00058089	904	27:05.8

TABLE A.2
Results for $0.5(H_{\omega_1,\omega_2}(G) + A(G))$.

Region	$\alpha\_$	$ITER$	Elapsed time
Hav30	0.08032077	61	00:40.3
Hav40	0.04599097	54	01:04.8
Hav50	0.04072380	82	02:32.2
Cat30	0.01977821	60	00:39.6
Cat40	0.04328554	75	01:26.5
Cat50	0.01731575	87	02:36.6
Eng30	0.01957200	76	00:54.3
Eng40	0.01351629	103	01:57.8
Eng50	0.00451793	128	03:46.9
Ucha30	0.02418143	46	00:28.8
Ucha40	0.05311207	66	01:14.3
Ucha50	0.04237537	49	01:29.8
Sud30	0.01937774	37	00:21.9
Sud40	0.04068631	45	00:50.9
Sud50	0.02852557	60	01:45.3
Mex30	0.00092313	201	02:17.7
Mex40	0.00105644	369	07:07.4
Mex50	0.00056019	524	15:40.6

TABLE A.3
Results for $0.5(S_t(G) + L(G))$.

Region	$\alpha\_$	$ITER$	Elapsed time
Hav30	0.00082193	62	00:40.6
Hav40	0.00013509	62	01:12.7
Hav50	0.00028982	73	02:19.9
Cat30	0.00020549	70	00:44.4
Cat40	0.00004959	74	01:22.8
Cat50	0.00006397	102	03:00.5
Eng30	0.00010500	76	00:50.2
Eng40	0.00019531	66	01:13.8
Eng50	0.00001290	96	02:48.6
Ucha30	0.00136186	56	00:37.6
Ucha40	0.00227402	70	01:20.0
Ucha50	0.00585372	77	02:22.8
Sud30	0.00213375	35	00:22.0
Sud40	0.01895250	35	00:39.1
Sud50	0.00771273	42	01:11.5
Mex30	0.00000001	201	02:13.0
Mex40	0.00002083	269	05:01.9
Mex50	0.00000001	312	09:40.4

TABLE A.4
Results for $0.5(S_{t,\omega}(G) + L(G))$.

Region	$\alpha\_$	$ITER$	Elapsed time
Hav30	0.00021352	50	00:32.5
Hav40	0.00004302	73	01:22.8
Hav50	0.00020498	65	02:02.0
Cat30	0.00015662	61	00:37.5
Cat40	0.00020840	50	00:56.8
Cat50	0.00041848	80	02:19.5
Eng30	0.00010222	59	00:40.2
Eng40	0.00008112	53	01:03.0
Eng50	0.00001024	101	02:57.4
Ucha30	0.00358187	38	00:25.7
Ucha40	0.00127044	42	00:46.8
Ucha50	0.00325217	46	01:22.4
Sud30	0.00200056	24	00:15.9
Sud40	0.02013530	35	00:36.9
Sud50	0.00680398	41	01:13.7
Mex30	0.00000103	163	01:44.3
Mex40	0.00001649	290	05:19.7
Mex50	0.00000001	331	09:59.6

Acknowledgment. Many thanks are due to the reviewers of this paper for their always valuable suggestions and comments.

REFERENCES

[1] P. Barrera-Sánchez, L. Castellanos, F. J. Domínguez-Mota, G. F. González-Flores, and A. Pérez-Domínguez, *Adaptive discrete harmonic grid generation*, Math. Comput. Simulation, 79 (2009), pp. 1792–1809.

[2] P. Barrera-Sánchez, L. Castellanos, F. J. Domínguez-Mota, G. F. González-Flores, and A. Pérez-Domínguez, *Area functionals for high quality grid generation*, in Proceedings of the 4th International Congress on Numerical Methods in Engineering and Applied Sciences, 2007.

[3] P. Barrera-Sánchez, L. Castellanos, and A. Pérez-Domínguez, *Métodos variacionales discretos para la generación de mallas*, Technical report, DGAPA-UNAM, Mexico City, Mexico, 1994.

[4] P. Barrera-Sánchez, F. J. Domínguez-Mota, and G. F. González-Flores, *Robust discrete grid generation on plane irregular regions*, Comput. Math. Math. Phys., 43 (2003), pp. 845–853.

[5] J. E. Castillo, ed., *Mathematical Aspects of Numerical Grid Generation*, Frontiers Appl. Math. 8, SIAM, Philadelphia, 1991.

[6] A. A. Charakhch'yan and S. A. Ivanenko, *A variational form of the winslow grid generator*, J. Comput. Phys., 135 (1997), pp. 385–398.

[7] A. A. Charakhch'yan and S. A. Ivanenko, *Curvilinear grids of convex quadrilaterals*, U.S.S.R. Comput. Math. and Math. Phys., 28 (1988), pp. 126–133.

[8] S. A. Ivanenko, *Harmonic mappings*, in Handbook of Grid Generation, CRC Press, Boca Raton, FL, 1999, pp. 8.1–8.41.

[9] P. M. Knupp and N. Robidoux, *A framework for variational grid generation: Conditioning the Jacobian matrix with matrix norms*, SIAM J. Sci. Comput., 21 (2000), pp. 2029–2047.

[10] P. Knupp and S. Steinberg, *Fundamentals of Grid Generation*, CRC Press, Boca Raton, FL, 1994.

[11] C.-J. Lin and J. J. Moré, *Newton's method for large bound-constrained optimization problems*, SIAM J. Optim., 9 (1999), pp. 1100–1127.

[12] S. Steinberg and P. J. Roache, *Variational grid generation*, Numer. Methods Partial Differential Equations, 2 (1986), pp. 71–96.

[13] J. G. Tinoco-Ruiz and P. Barrera-Sánchez, *Area functionals in plane grid generation*, in Proceedings of the 6th International Conference on Numerical Grid Generation in Computational Field Simulation, London, England, International Society of Grid Generation, Mississippi State, MS, 1998, pp. 293–302.

[14] J. G. Tinoco-Ruiz and P. Barrera-Sánchez, *Smooth and convex grid generation over general plane regions*, Math. Comput. Simulation, 46 (1998), pp. 87–102.

[15] Unamalla, *An Automatic Package for Numerical Grid Generation*, http://www.matematicas.unam.mx/unamalla.

[16] A. M. Winslow, *Numerical solution of the quasilinear Poisson equations in a nonuniform triangle mesh*, J. Computational Phys., 1 (1967), pp. 149–172.

[17] C. Zhu, R. H. Byrd, and J. Nocedal, *Algorithm* 778: *L-bfgs-b: Fortran routines for large-scale bound-constrained optimization*, ACM Trans. Math. Software, 23 (1997), pp. 550–560.